VISUAL STUDIES ON THE WAKE OF A ROUGHNESS ELEMENT PROXIMATE TO A WALL

YOSHIMASA FURUYA and MASAFUMI MIYATA

Department of Mechanical Engineering

(Received October 27, 1972)

I. Introduction

When a solid surface over which fluid flows is not hydrodynamically smooth, the frictional resistance and the transition from laminar to turbulent flow depend on the geometrical shape of roughness elements and their spacial arrangement. In particular, when roughness elements have three-dimensional shape, the flow pattern around them becomes very complex. To obtain a proper understanding of such a flow field, it is important, at first, to investigate its nature qualitatively by means of flow visualization.

There are many investigations on the wake of a two-dimensional obstacle in uniform flow in a fairly wide range of Reynolds number, fewer for the case of a wake of three-dimensional obstacle. Magarvey and Bishop[1] investigated the flow around a liquid drop descending in water and Goldburg and Florsheim[2] observed the same phenomenon using solid bodies of different shape. Little is known about a detailed structure of the wake of an obstacle on the wall, for almost all investigators have focussed attention on flow transition phenomenon due to the obstacle, where an interesting experiment using flow visualization method was carried out by Schultz-Grunow[3]. This report is concerned with visual studies on the wake of roughness elements proximate to a wall.

With a wall or a boundary layer flow, it can be expected that the flow around the three-dimensional obstacle on a wall is different from that in uniform flow. In this case, in addition to the vortex formed periodically in the wake which is similar to Kármán vortex, steady vortices which are fixed to the obstacle and have their axes in the streamwise direction (necklace-vortex) are formed. In this experiment, the wake of two or three-dimensional roughness element was investigated using the water channel on the bottom of which laminar boundary layer was formed. Emphasis was put on the observation of wake pattern with the change of aspect ratio of roughness elements.

The following results were obtained. For the case of a three-dimensional roughness, when aspect ratio is small, there exists some Reynolds number range over which vortex-loops are formed periodically in the wake, but this range becomes smaller with increasing aspect ratio. For the two-dimensional case, the formation of such stable vortex-loops was observed hardly at all.

Effects of a wall or a sheared flow on the vortex formation around the two-dimensional circular cylinder were also investigated, where circular cylinders of different diameter were placed near or within the boundary layer.

Nomenclature

x : coordinate axis parallel to the channel center line
d : diameter of a circular cylinder or a sphere
l : circular cylinder length
δ : boundary layer thickness
u : streamwise component of the velocity inside boundary layer
ν : kinematic viscosity
St : Strouhal number, $f \cdot d/U$ or $f \cdot d/u$
y : coordinate axis normal to the bottom wall
h : distance from the bottom wall where a circular cylinder is placed
U : velocity outside boundadary layer
f : vortex shedding frequency
Re: Reynolds number, $U \cdot d/\nu$ or $u \cdot d/\nu$

II. Experimental apparatus and procedure

(*1*) *Water channel* To use flow visualization technique in water channel flow, it is very important to obtain a sufficiently steady and two-dimensional flow in a channel. Fig. 1 shows the schematic arrangement of the water channel used in this experiment. The measuring section consists of perspex glass plates making a rectungular cross-section of 290×295 mm and 1.4 m long. The contraction parts used at first are shown in Fig. 2–a, where both side and bottom wall of it consisted of curved plates making rather strong contraction, and then secondary currents appeared near the corners. These secondary currents, however, could be weakened enough by employing the contraction with an almost straight wall and by care in shaping the settling-chamber as shown in Fig. 2–b. Fig. 3 shows the visualized flow near the bottom wall obtained by means of hydrogen-bubble method. The velocity profile calculated from this well agrees with Blasius-profile (Fig. 4). The two-dimensionality of the channel flow is quite good as shown in Fig. 5, where the bubble generating wire is located about 70 mm above the bottom wall.

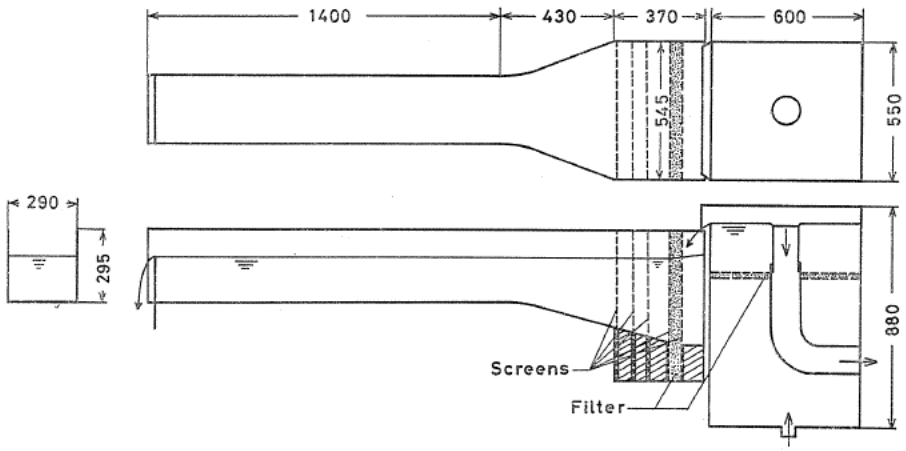

FIG. 1. Schematic arrangement of the water channel.

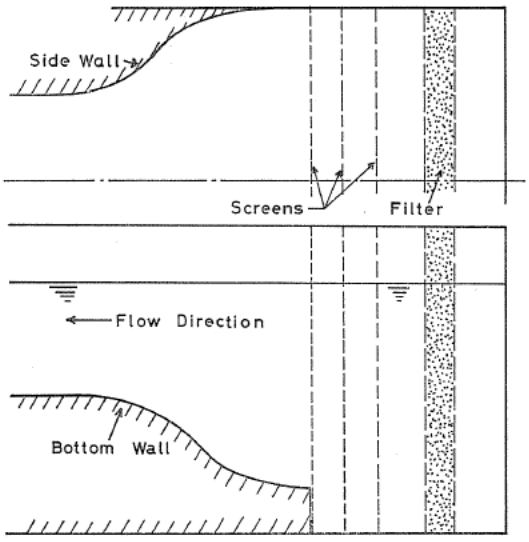

FIG. 2-a. Unsuitable configuaration of a contraction and a setlling chamber.

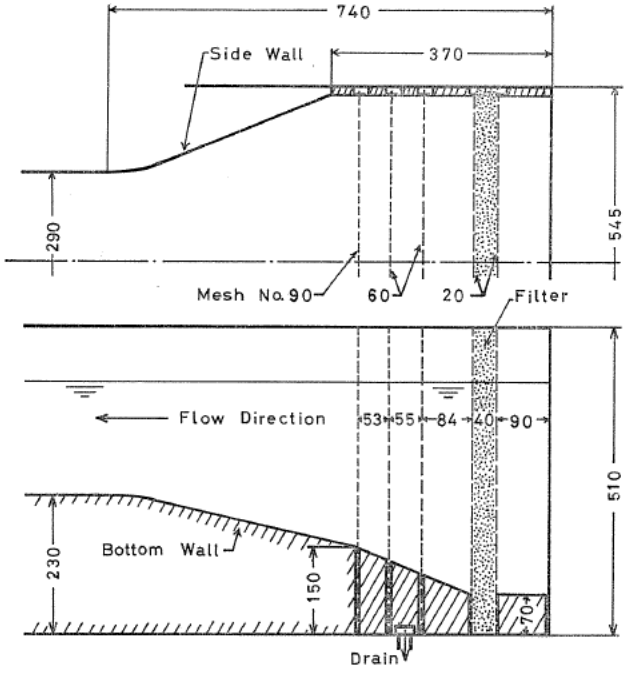

FIG. 2-b. Details of the contraction and the setlling chamber employed.

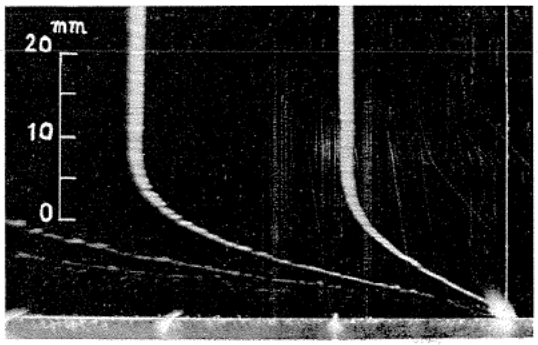

FIG. 3. Visualized boundary layer flow. The bubble generating wire is placed normal to the bottom wall at the center of the water channel.

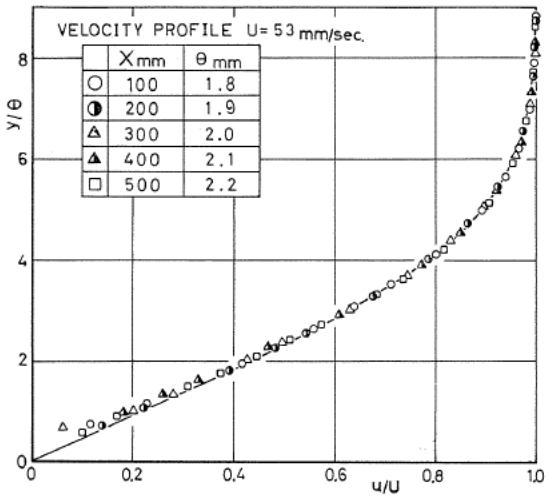

FIG. 4. Blasius profile.

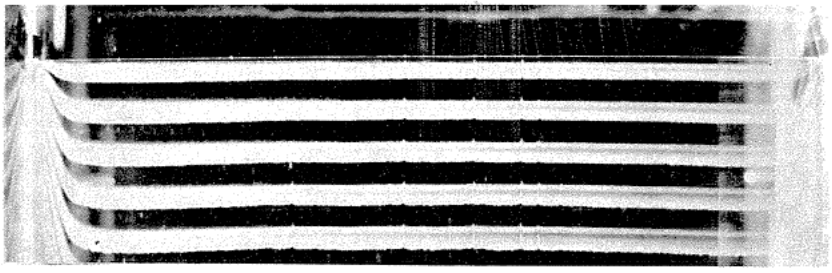

FIG. 5. Visualized transverse velocity profile. The flow direction is from top to bottom, where the wire is placed normal to the flow and parallel to the bottom wall at $y=70$ mm.

(*2*) *Flow visualization method* To observe a flow field, hydrogen bubble and two kinds of dye were used as a tracer. The hydrogen bubble method utilizes the electrolysis of water between two electrodes. In this experiment, negative-electrode is 100 μ platinum wire and positive-electrode is thin blass plate and hydrogen bubbles are generated in the negative-electrode. The generation of bubbles may be controlled freely by a electric pulse generator, so it facilitates quantitative flow analysis. The pulse generator has the voltage range of 0~200 V, pulse repeat range of 0.05~5.0 sec and pulse width range of 0.01~1.0 sec, and these can be changed continuously. Hydrogen-bubbles are dissoluble in water, therefore, it is not covenient for observation over a wide area. In this respect, dye injection method is more suitable. Therefore, in the main, to observe the wake flow the latter was employed. The dyes used were Fluorescentnatrium and Rodamin-B, and the respective solutions of proper concentration were injected into the flow through hypodemic tubes.

Observation was conducted by placing a circular cylinder normal to the flow and parallel to the bottom wall at different distances from it, where circular cylinders of three kinds of diameter (d=1.8, 3.5 and 6.0 mm) were used. Observation was also conducted when a sphere of 10 mm diameter or a short circular cylinder of 10 mm diameter with different aspect ratio was placed on the bottom wall center. Flow velocity can be measured from the photograph of the flow visualized by hydrogen bubble method.

III. Experimental results and discussion

(*1*) *Effects of boundary layer on the vortex street of a circular cylinder* In Fig. 6 a circular cylinder is placed normal to the flow and parallel to the bottom wall at a distance of $h=3\,\delta$ from the bottom. Reynolds number based on the velocity 100 mm upstream of the cylinder center is about 70. The whole flow field and Strouhal number are almost the same as that in uniform flow, but the distance between two rows of vortices is a little increased and space-ratio (distance between vortices to distance between rows) becomes about 0.42. Figs. 7-a~d shows the case where h and d are constant and velocity is increased (δ is decreased). In Fig. 7-a a cylinder is located at almost the outer edge of the boundary layer, namely $h/\delta=1$, and the lower row of vortices enters into the boundary layer so that the wake pattern differs somewhat from that in uniform flow, but the vortex street remains stable over the whole length of the water channel. When $h/\delta\sim1$,

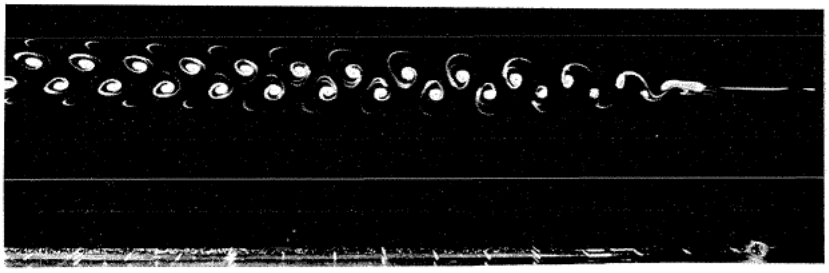

FIG. 6. $Re=70$: $d=3.5$ mm, $h=63$ mm.

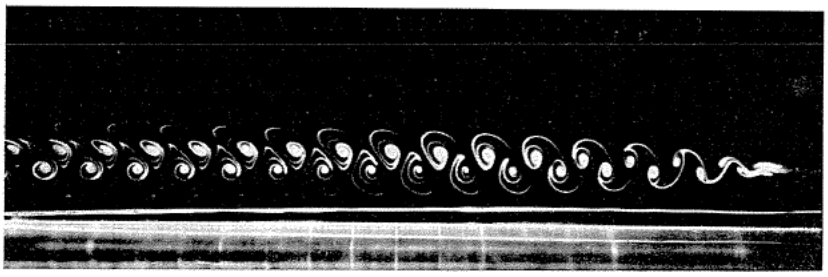

(a) $Re=55$

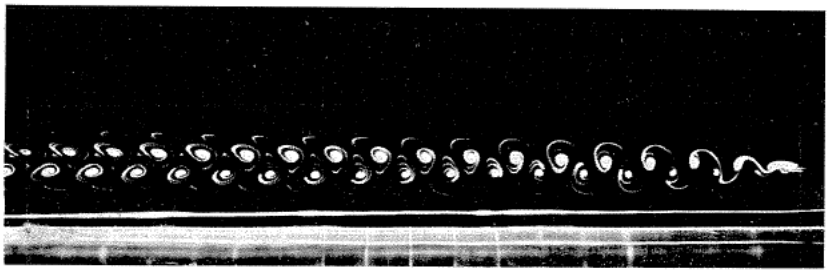

(b) $Re=70$

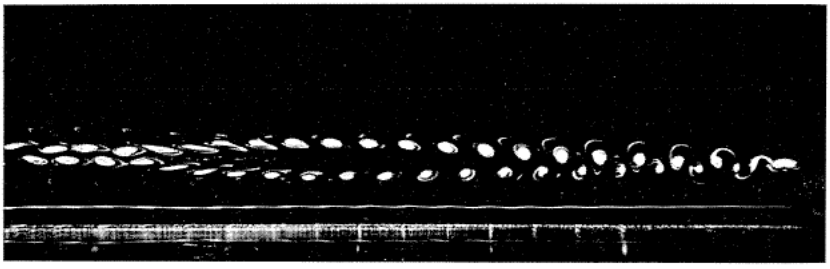

(c) $Re=110$

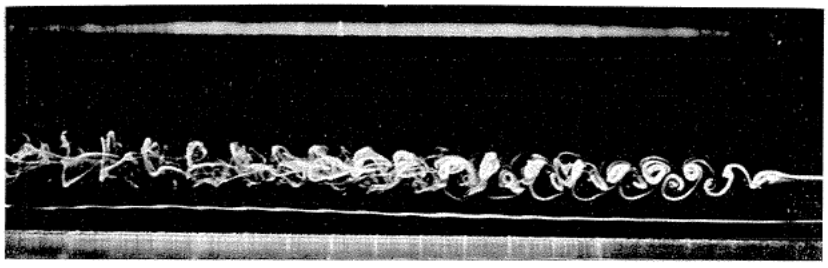

(d) $Re=140$

FIG. 7. $d=3.5$ mm, $h=29$ mm.

as in Fig. 7-b, the cylinder is a little outside the boundary layer, the whole flow pattern becomes similar to that in uniform flow. At $h/\delta=1.8$ and $Re=110$ there appeared the periodic change of the distance between rows (Fig. 7-c). This phenomenon is very similar to that found by Tritton[4] in uniform flow at $Re=90$. Transition to turbulent flow takes place somewhat earlier. At $Re=140$ vortex street becomes irregular as shown in Fig. 7-d. Fig. 8 shows the case where $h/\delta=0.9$ and $Re=50$. Effects of sheared flow appear clearly in the vortex pattern, where translational velocities of each row differ obviously. In spite of this the vortex street is comparatively stable. As h/δ becomes smaller, namely, when cylinder is deeply immersed in the boundary layer, vortex street takes on a characteristic arrangement due to the different translational velocities of each row as shown in Figs. 9-a, b. Another characteristic feature of vortex street proximate to the wall is described as follows. As Reynolds number increases, the distance between rows becomes very small and vortex street appears as if

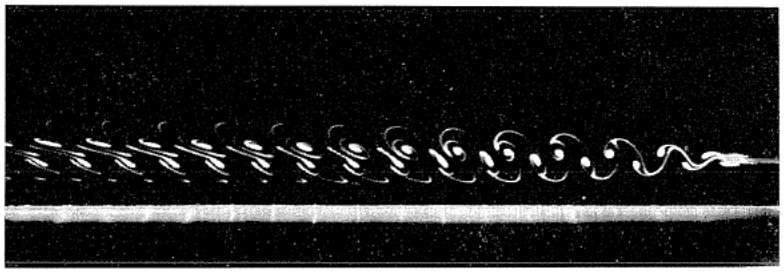

FIG. 8. $Re=50$: $d=3.5$ mm, $h=24$ mm.

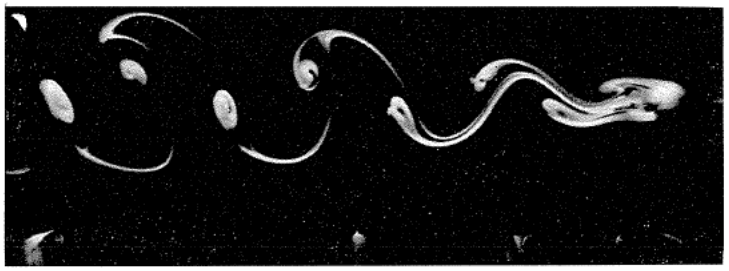

FIG. 9-a. $Re=60$: $d=3.5$ mm, $h=18$ mm.

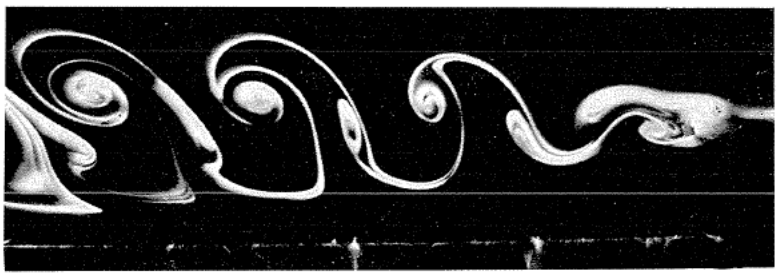

FIG. 9-b. $Re=90$: $d=3.5$ mm, $h=13$ mm.

there was only one row over a fairly long dictance downstream from the cylinder (Fig. 10, $Re=130$). This feature persists after the vortex street becomes turbulent.

Using observational results described above, the dimensionless frequency of vortex shedding St are plotted against Re in Fig. 11, where characteristic velocity is the value at 100 mm upstream of the cylinder center as mentioned before. The two curves in this figure show the empirical relation of Roshko[5] in uniform flow corresponding to $50<Re<150$ and $300<Re<3000$. Using this characteristic velocity, the results agree well with Roshko's relation over a rather wide range of Reynolds number, in spite of the modified vortex pattern due to sheared flow. The value of the critical Reynolds number in this experiment is about 40, which is nearly the same value of that in uniform flow. However, when h/δ becomes smaller, the value of St becomes larger than that given by Roshko's relation in the lower range of Reynolds number. This trend becomes clear as h/d becomes smaller. For the case of the cylinder approching the limit, as when placed on the wall, the value of St becomes extremely large. For example, when $Re=40$ and 80, Strouhal number is about 0.6 and 0.3 respectively, which is several times as large as that in uniform flow. Therefore, the vortex in this condition can be considered to have an entirely different nature from that of Kármán vortex.

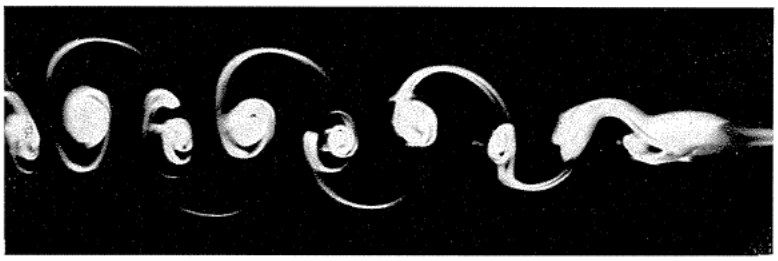

FIG. 10. $Re=130$: $d=3.5$ mm, $h=18$ mm.

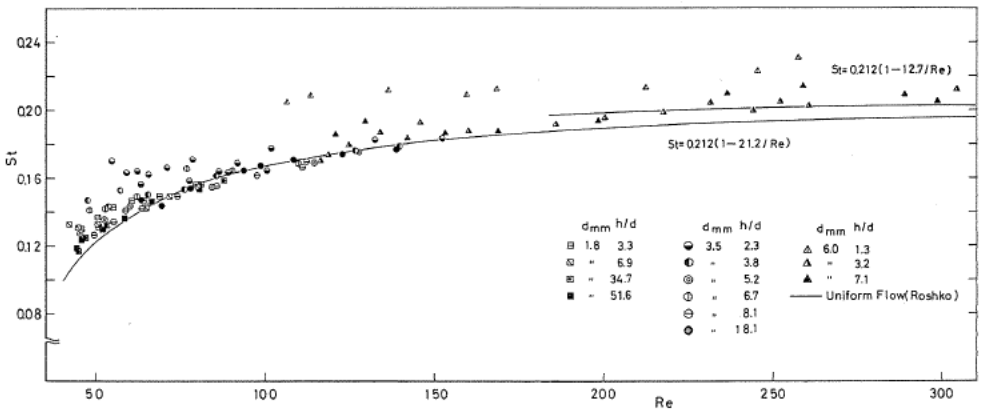

FIG. 11. Effects of a wall or boundary layer on Strouhal numbers for a circular cylinder proximate to a wall. Characteristic velocity is the value at 100 mm upstream of the cylinder center.

Vortices around the cylinder placed on the wall will be discussed in a subsequet section.

(2) Vortices around the three-dimensional roughness at the wall

In the previous section it was mentioned that vortices around the two-dimensional cylinder placed on the wall have quite different features from that in uniform flow. Experiments were conducted with three-dimensional roughness such as sphere and short circular cylinder as well as the two-dimensional type on the wall. Fig. 12 shows the relative dimensions of roughness height d to the boundary layer thickness δ. The ratio d/δ takes the value of about 1 at the higher velocity and about 0.5 at the lower. In the following discussions, the characteristic velocity means the velocity at the roughness height 100 mm

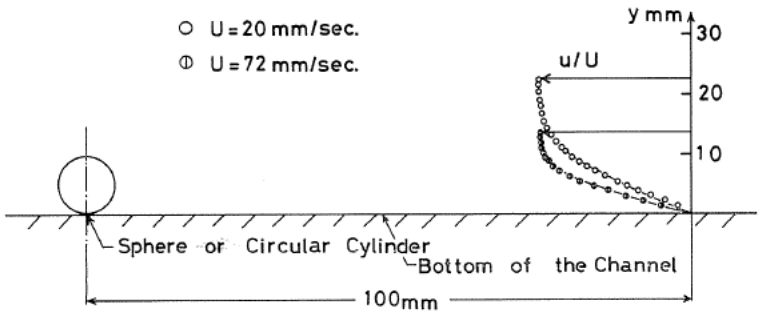

FIG. 12. Relative dimensions of a roughness height to boundary layer thicknesses.

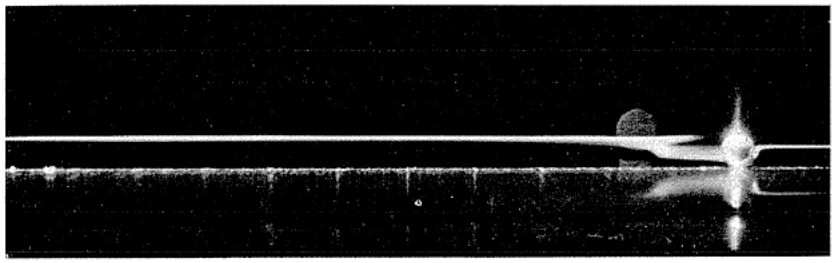

FIG. 13-a. Sphere: $Re=280$.

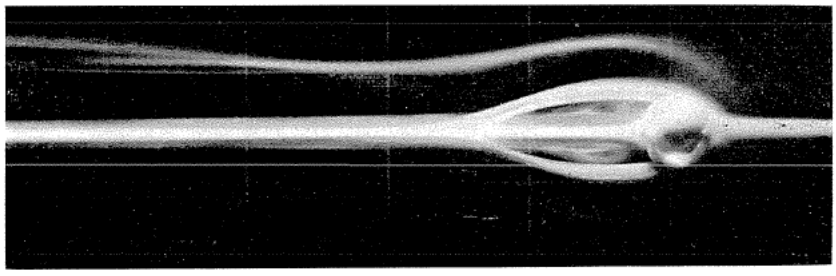

FIG. 13-b. Sphere: $Re=280$.

upstream from the roughness, contrary to that at its center as in the foregoing section. The reason for it will be explained later.

(*a*) *Flow around a spere* Figs. 13-a, b show the flow around the sphere at $Re=280$, as seen from above and the side respectively. The wake does not show any oscillation and a stable thread-like wake is observed. With increasing Reynolds number, this thread-like wake becomes wavy and beyond a certain critical value, regularly arranged vortex-loops are formed (Figs. 14-a, b $Re=500$). Another vortex tube streching downstream from both sides of the sphere (necklace-vortex) is seen to exist as in Fig. 14-a. This vortex is caught up into by the above-mentioned vortex-loops. At still higher value of *Re*, vortex-loops are shed irregularly and the wake becomes turbulent where so-called "horse-shoe" type vortices still can be seen clearly.

(*b*) *Flow around a short circular cylinder* (b-1) $l/d=1$; Figs. 16-a, b show the flow around the circular cylinder of aspect ratio of 1 at $Re=160$. Quite

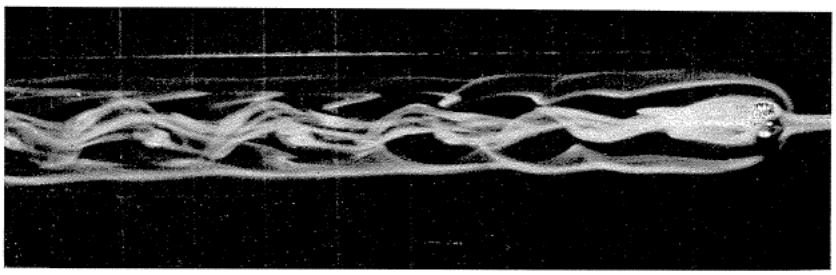

FIG. 14-a. Sphere: $Re=500$.

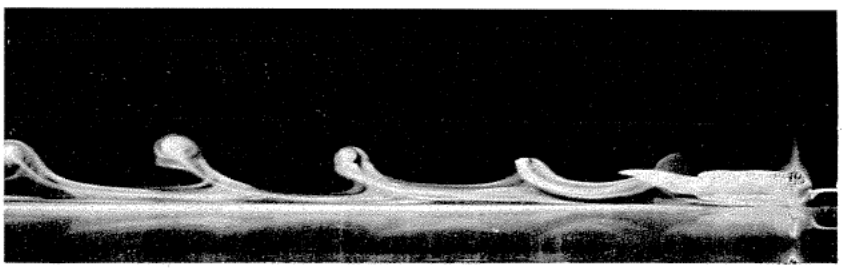

FIG. 14-b. Sphere: $Re=500$.

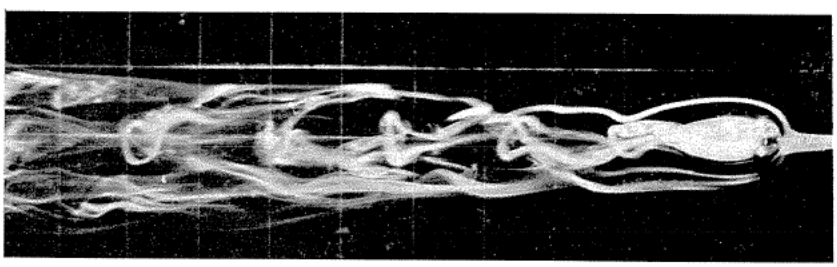

FIG. 15. Sphere: $Re=690$.

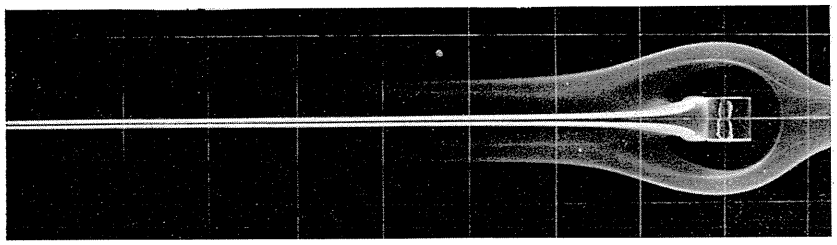

FIG. 16-a. Circular cylinder of $l/d=1$: $Re=160$.

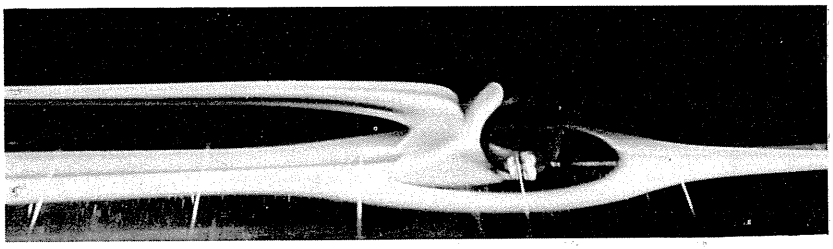

FIG. 16-b. Circular cylinder of $l/d=1$: $Re=160$.

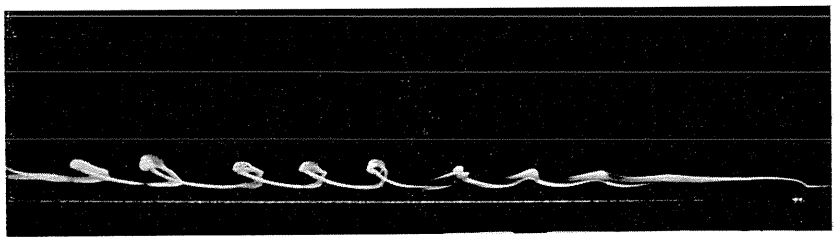

FIG. 17-a. Circular cylinder of $l/d=1$: $Re=290$.

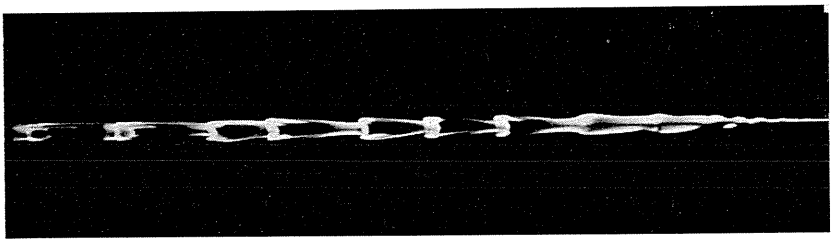

FIG. 17-b. Circular cylinder of $l/d=1$: $Re=290$.

similarly to the case of a sphere, the wake dose not oscillate till a critical Reynolds number and above this value vortex-loops are formed regularly in the wake. In this case vortex-loops are more stable than that of a sphere (Figs. 17-a, b $Re=290$), probably due to the definite separation line at the both sides. Figs. 18-a, b show the flow in the plane of symmetry at the successive station at $Re=190$, 690 respectively, where the flow is visualized by hydrogen bubble method.

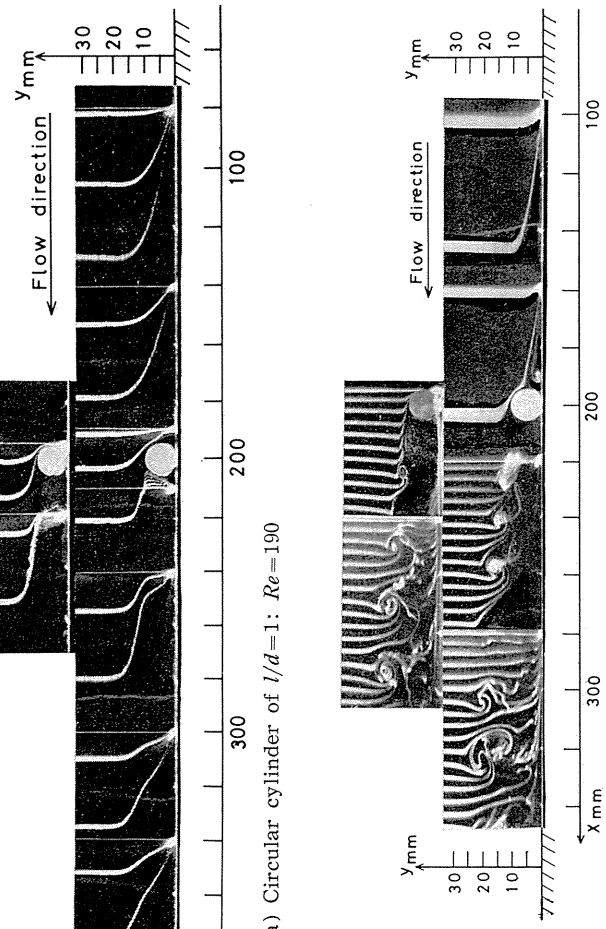

(a) Circular cylinder of $l/d=1$: $Re=190$

(b) Circular cylinder of $l/d=1$: $Re=690$

FIG. 18. Flow along the plane of symmetry. The flow is visualized by hydrogen bubble method.

(b-2) $l/d=3$; When the aspect ratio of cylinder is increased, the formation of vortex-loops takes place at comparatively small value of Re and vortex-loops tend easily to deform. Fig. 19 shows the case where $l/d=3$ and $Re=150$. The flow in Fig. 20 is seen from above at $Re=230$. Necklace-vortex and the way in which there is the phenomenon of being caught up by the vortex-loops can be seen clearly. This necklace-vortex becomes stronger as Reynolds number is increased and above a certain value, two comparatively strong vortices can be

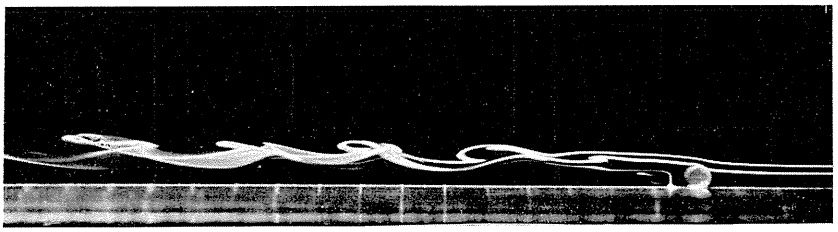

FIG. 19. Circular cylinder of $l/d=3$: $Re=150$.

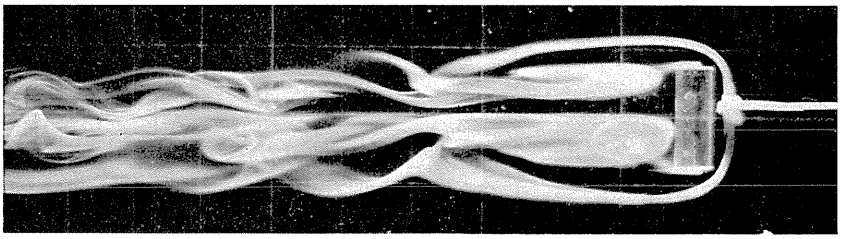

FIG. 20. Circular cylinder of $l/d=3$: $Re=230$.

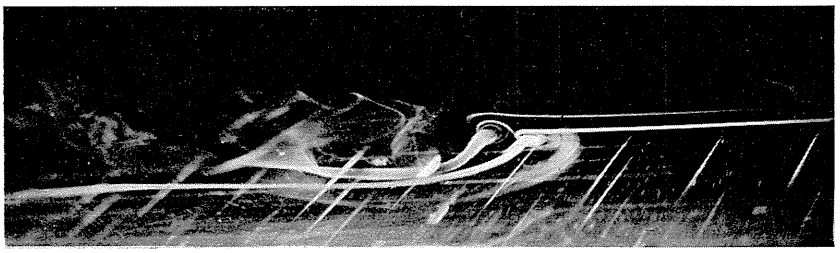

a

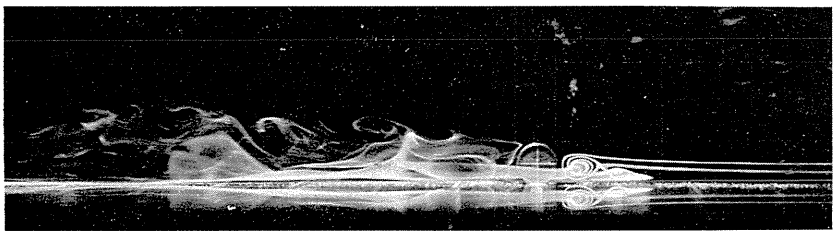

b

FIG. 21. Circular cylinder of $l/d=3$: $Re=480$.

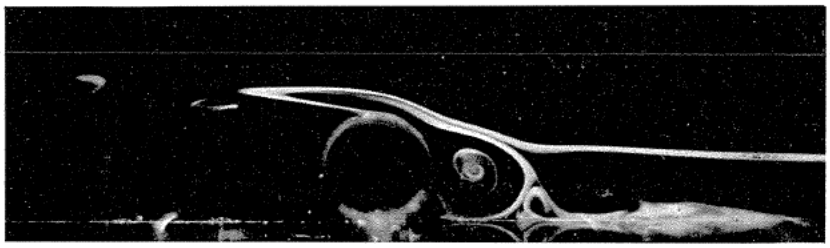

FIG. 22. Circular cylinder of $l/d=3$: $Re=615$.

FIG. 23. Circular cylinder of $l/d=6$: $Re=180$.

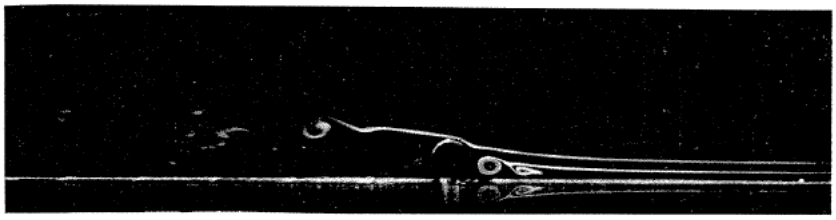

FIG. 24. Circular cylinder of $l/d=6$: $Re=575$.

FIG. 25. Circular cylinder of $l/d=\infty$: $Re=180$.

observed (Fig. 21, $Re=480$). At still higher value of Re, these begin to oscillate up and down and the fluid being captured by the stronger vortex jumps over the cylinder (Fig. 22, $Re=615$).

(b-3) $l/d=6$; When $l/d=6$, as shown in Fig. 23, the vortex-loops become very unstable and easily break down. At $Re=575$ the wake becomes turbulent and just upstream of the cylinder there exist two strong necklace-vortices as in Fig. 24.

(b-4) $l/d=\infty$; Fig. 25 shows the flow around the two-dimensional cylinder on the wall at $Re=180$. Even at such a small Reynolds number, regular vortex-

loops can not be observed. There exist only several irregularly formed vortex-loops which are unstable and have three-dimensionality. The instability of the vortex system in this case can be explained by the instability of the symmetrical double rows of two-dimensional vortices which occur when the wall is replaced by image system.

(3) Change of wake pattern with Reynolds number

From aforesaid observations, types of the wake patterns around the circular cylinder on the wall are brought together in Fig. 26, where the ordinate is the reciprocal of aspect ratio d/l and the abscissa is Reynolds number. As shown in this figure, there exist three patterns of wake (stable thread-like wake, regular vortex-loop configuration and irregular vortex-loop configuaration) corresponding to that of uniform flow. The critical Reynolds number at which vortex-loops begin to be formed regularly in the wake increases with decreasing aspect ratio. It is the same with the Reynolds number range over which regular formation of vortex-loops are observed. A sphere takes a little smaller critical value, as compared with the circular cylinder of the aspect ratio of 1.

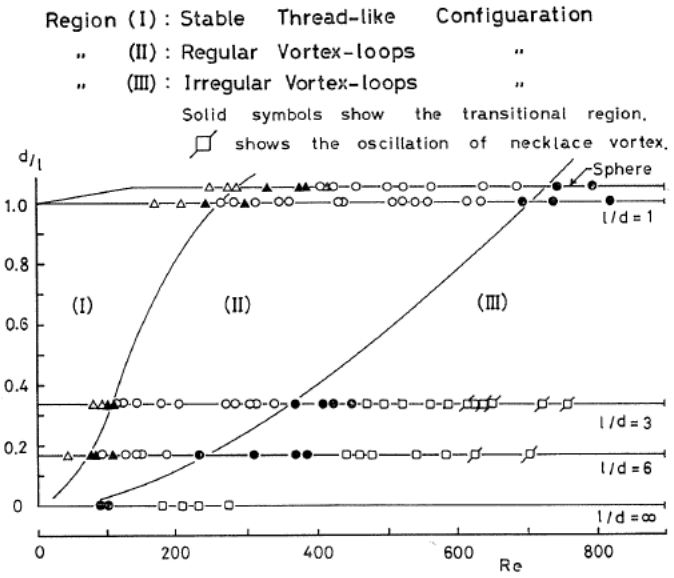

FIG. 26. Change of wake pattern with Reynolds number.

(4) Relations between Strouhal number and aspect tatio

In Fig. 27 the dimensionless shedding frequency of vortex-loops is plotted against Reynolds number. A curve in this figure shows the empirical relation of Goldburg and Florsheim[2] obtained for the sphere in uniform flow. Using the velocity at the roughness height and 100 mm upstream of the roughness as the characteristic velocity, the results with a sphere in this experiment nearly agreed with this curve. Therefore, the results with a circular cylinder were also plotted employing the same velocity. It can be seen from this figure that Strouhal

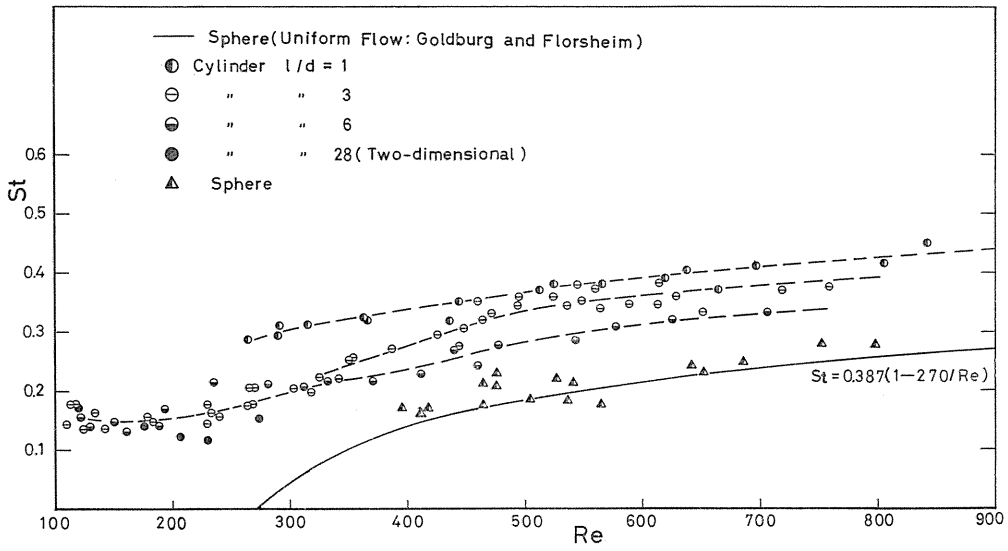

FIG. 27. Effects of aspect ratio on Strouhal numbers for the roughness element placed on the wall. Characteristic velocity is the value at the roughness height and 100 mm upstream of the roughness element.

number for a circular cylinder is larger than that for a sphere, but it approaches that of a sphere with increasing aspect ratio. It is worth notice that the cylinder of aspect ratio of 1 which has a shape most similar to a sphere attains almost twice the value of the sphere.

IV. Concluding remarks

The vortex system behind the two-dimensional circular cylinder proximate to the wall is stable till a certain critical Reynolds number which is a little smaller than that in uniform flow. Arrangement of the vortices is modified by the sheared flow, but Strouhal number using the velocity proposed here becomes almost the same as that in uniform flow.

When the three-dimensional obstacle is placed on the wall, there also exists some Reynolds number range over which vortex-loops are formed periodically, but this range becomes smaller with increasing aspect ratio of the cylinder, then the formation of a stable vortex system was observed hardly at all for the two-dimensional case. Strouhal number in this case depends on not only aspect ratio but also on the shape of the obstacle.

References

1) Magarvey, R. H. and Bishop, L., Canad. J. of Phys., **39**, 1961.
2) Goldburg, A. and Florsheim, B. H., Phys. Fluid, **9**, 1966.
3) Schultz-Grunow, F., Z. AMM, **38**, 1953.
4) Tritton, D. J., J. Fluid Mech., **6**, 1959.
5) Roshko, A., NACA Rep., 1954.